Title
DYNAMIC SIMILITUDE IN SCALE MODELS OF BUILDINGS

Authors
Richardson, R.W.
Berman, S.M.

Publication Date
1981-08-01

LBL-13262
Preprint

Lawrence Berkeley Laboratory
UNIVERSITY OF CALIFORNIA

ENERGY & ENVIRONMENT DIVISION

Submitted to the International Journal of Heat and Mass Transfer

DYNAMIC SIMILITUDE IN SCALE MODELS OF BUILDINGS

R.W. Richardson and S.M. Berman

August 1981

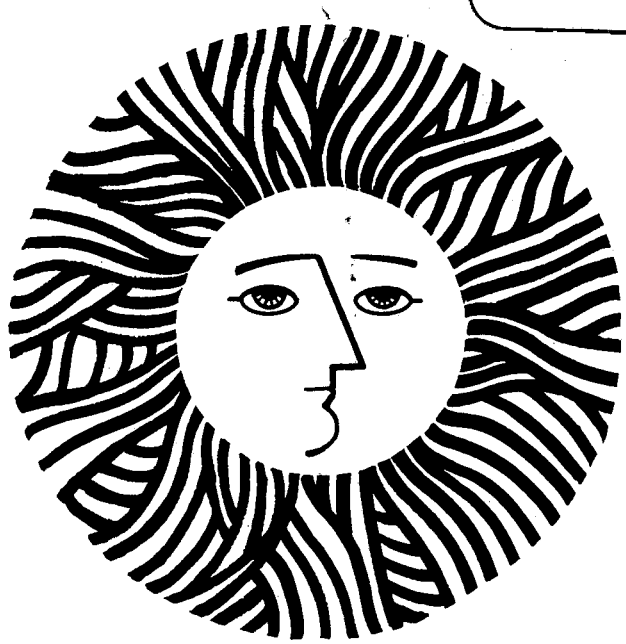

Prepared for the U.S. Department of Energy under Contract DE-AC03-76SF00098

DISCLAIMER

Submitted to International Journal
of Heat and Mass Transfer

LBL-13262

DYNAMIC SIMILITUDE IN SCALE MODELS OF BUILDINGS

R. W. Richardson* and S. M. Berman

Energy Efficient Buildings Program
Lawrence Berkeley Laboratory
University of California
Berkeley, California 94720

August, 1981

This work was supported by the Assistant Secretary for Conservation and Renewable Energy, Office of Buildings and Community Systems, Buildings Division of the U.S. Department of Energy under Contract No. DE-AC03-76SF00098.

---

*Permanent address, Physics Department, New York University, New York, NY 10003.

ABSTRACT

Conditions for dynamic thermal similarity of a small-scale building (scaled in both spatial and temporal dimensions) with its full-scale counterpart (fully sized and evolving in real time) are derived. The conditions ensure proper scaling of conductive, radiative, and convective transport of thermal energy. The restrictions imposed by these conditions are discussed and exemplified with a small-scale model in a Xenon atmosphere at standard temperature and pressure and one in a sulfur hexafluoride atmosphere at an elevated temperature and standard pressure. It is shown that it is possible to construct models having small physical sizes and accelerated temporal data rates for the exact analog simulation of the thermal performance of buildings.

SYMBOL LIST

Symbol	Meaning	Equation where first used
a	Scaling variable, α'/α	(2.24)
c	Specific heat	(2.1)
g	Acceleration of gravity	(2.7)
k	Thermal conductivity	(2.1)
k_B	Boltzmann constant	(D.3)
l	Scaling variable, L'/L	(2.23)
n	Scaling variable, ν'/ν	(2.24)
$\dot{n}$	Scaling variable, $\dot{N}'/\dot{N}$	(2.37)
p	Scaling variable, P_o'/P_o	(2.26)
t	Scaling variable, T_o'/T_o	(2.22)
y	Proportion of two-component wall	(E.3)
$\vec{v}$	Velocity field	(C.1)
C	Heat capacity per unit volume	(2.12)
E	Radiant energy flux	(B.1)
G	Incident radiant flux	(B.3)
Gr	Grashoff number	(2.7)
H	Heat rate from a point source	(2.36)
$\vec{H}$	Conductive heat flux	(D.10)
J	Net radiant flux	(B.3)
$J_{o,1}$	Thermal fluxes	(E.7)
L	Characteristic length	(2.2)
M	Mean molar mass	(2.8)
$\dot{N}$	Infiltration rate	(2.37)

SYMBOL LIST (continued)

Symbol	Meaning	Equation where first used
P	Pressure	(2.19)
P_r	Prandtl number	(2.6)
P_{xy}	Fluid stress tensor	(D.1)
R	Thermal resistivity	(E.4)
S	Solar flux	(2.33)
T	Temperature	(2.5)
ΔT	Amplitude of temperature variation	(2.7)
U	Wall U-value, k/l	(2.12)
α	Thermal diffusivity	(2.1)
γ	Scaling variable, $\rho' c_p'/\rho c_p$	(3.7)
δ	Scaling variable, $\Delta T'/\Delta T$	(2.22)
ϵ	Emittance of surface	(2.4)
η	Scaling variable, H'/H	(2.36)
κ	Scaling variable, k'/k	(2.24)
μ	Dynamic shear viscosity	(C.2)
ν	Kinematic shear viscosity	(2.6)
ρ	Mass per unit volume	(2.1)
σ	Scaling variable, S'/S	(2.34)
τ	Scaling variable, τ_ω'/τ_ω	(3.1)
$\tau_{\omega,f}$	Characteristic time	(2.12)
ω	Angular frequency	(E.7)
χ	Thermal response factor	(E.7)
ζ	Bulk viscosity	(C.2)

SYMBOL LIST (continued)

Subscripts	Meaning
w	Wall
f	Fluid
s	Gas property under standard conditions
o	Average value
p	Constant pressure
i	Layer index in wall

Subscripts	
'	prime: small-scale model
	no prime: full-scale model

1. Introduction

There are three quantitative methods for learning about the thermal performance of a building or other complex structure. They are

1. Build the building and then observe its actual performance.
2. Perform a numerical simulation of the performance of the building on a computer.
3. Build a small-scale model of the building, observe its performance, and scale the results up to full-scale size.

The first method is not generally practical since it may be excessively costly and require long periods of time with corrections both difficult and expensive to incorporate. The second method is of questionable reliability due to the many uncontrolled approximations that underlie any such numerical simulation. The third method has not been fully exploited; this paper is devoted to developing this method into a useful research and design tool.

Small-scale models of buildings have been used by architects to simulate the visual aspects and spatial relations of a proposed design for many years. However, such models have not been used extensively to simulate the thermal performance of the building. Some early work along this line was done in Australia after World War II.[1] In these studies, one-third and one-ninth scale models were used to study the effect of thermal mass on the diurnal temperature swing of a building. Studies on a one-quarter scale model of a cubic room have also been reported.[2] In both of these studies it was argued that since radiative (see Appendix B) and convective (see Appendix C) energy transport are independent of scale, then conductive transport (see Appendix A) also should not depend on scale. Thus the U-values of the walls should not be changed. This can be achieved by either not scaling the thickness of the wall or by using materials of low thermal conductivity. The first method violates

the 3-dimensional nature of the scaling; the second method is difficult to enact due to the limited range of properties of available materials. Furthermore, convective energy transport is independent of scale only in the domain of fully developed turbulent flow.[6] This may be marginally true for the full-scale buildings (which are characterized by Grashof numbers $\sim 10^{10}$), but is probably not true of the small-scale model. Furthermore, there was no temporal scaling in these studies because the small-scale model evolved in real time or only steady-state phenomena were investigated. Thus, the full potential of spatial and temporal scaling was not exploited.

The NASA space program provided further impetus for studying small-scale models. Here, the objective was to understand the thermal behavior of a spacecraft in an extraterrestial environment. The early work is reviewed by Vickers[3]; Shanon[4] has reported a study that is close to the spirit of the present work. He reports a fair agreement in a study of a one-quarter scale model having cylindrical symmetry.

A study having the same objective as the present work has been reported by Thompson, Han, and Azer.[5] They studied a one-eighth scale model of a four-bedroom town house that had been treated in full scale at the National Bureau of Standards. They report results that are within 10% of the temperature of the full-scale model. However, it is difficult to assess the validity of their use of forced rather free convection and their neglect of radiative energy transport in the operation and analysis of this model. Furthermore, since they have chosen to validate their methods on a complex structure, one cannot tell whether their 10% agreement is fortuitous or fundamental.

In the studies cited above, energy transport by convection is parameterized by semiempirical film coefficients or Nusselt numbers. We use

the more fundamental description contained in the Navier-Stokes equations and require that the small-scale model give a similarity solution to the full-scale building. We also allow the modification of a broader range of parameters such as the composition of the atmosphere, its temperature and pressure, etc., in order to achieve this similarity. In further contrast to these previous works, we include the temperature and pressure dependence of the transport coefficients of the gas (see Appendix D) in our scaling equations.

In summary, the past work on thermal models of buildings does not properly account for the interconnections between the properties of materials and spatial and temporal scaling while allowing all three thermal energy transfer mechanisms to fully participate.

The three processes of thermal energy transport, conduction, radiation, and convection, are of roughly equal importance in a typical building. This can be seen from the fact that radiation and convection contribute about equally to wall/film coefficients and these film coefficients are large compared to typical wall conductances. The films, of course, are exposed to smaller temperature differences than are the walls. Thus, any dynamically similar scale model must scale all the three transport processes properly. We address this scaling in Sec. 2, where we derive a set of six scaling relations that ensure that the small-scale model will be dynamically similar to the full-scale building. We have placed the technical details associated with this section in a series of appendices. Thus, conduction, radiation, and convection are treated in Appendices A, B, and C respectively and the mean-free-path expressions for the transport coefficients of a gas are discussed in Appendix D. The implementation of the scaling relations is discussed in Sec. 3. There we show by examples that interesting results can be obtained

using a Xenon atmosphere at room temperature and pressure or an SF_6 atmosphere at elevated temperature and standard pressure. However, we have not fully explored the possibility of using mixtures of gases. The discussion is given at two different levels. At the first level, we assume that heat conduction in the walls is one-dimensional, i.e., only in the direction perpendicular to the wall; at the second level we require full three-dimensional similarity. The assumption of one-dimensional heat conduction is used in every known numerical simulation and it is a virture of our formulation that we can build models with or without this assumption. We conclude with a discussion of some areas of future investigation in Sec. 4. Appendix E is devoted to the detailed design considerations of full- and small-scale boxes the thermal performances of which can be compared and used as a test of our scaling relations.

2. Scaling

We seek the definition of a small-scale model of a room or building that will be used to simulate the thermal performance of the full-sized version. The motiviations for such a search are twofold. First, since the scale model is assumed to be smaller than full size, construction will involve less material and the model will be more amenable to modification as measurements proceed. Second, shorter time scales are associated with smaller physical scales, resulting in a faster rate of data acquisition. The models we discuss in this section share both of these advantages.

The methods we use are common to classical hydrodynamics--we look for similarity solutions of the equations describing the system. The physical properties (such as length, temperature, pressure) in a similarity solution are related to those of the real solution by simple scale factors. Thus, if

we can find a similarity solution for the basic equations, we can build a small-scale model based on it and then determine the properties of the full-scale model by a simple scaling of the observed properties of the model.

The equations that we need to study are those describing thermal energy transport in an enclosed region. The mechanisms of energy transport are conduction, radiation, and convection; the equations describing these mechanisms are presented in detail in the appendices. Similarity solutions to these equations are obtained by changing the values of the characteristic parameters describing the system in such a way that the physical properties are scaled as described above. There are a total of ten such parameters for the systems that we are considering and, as an introduction to what follows, we will now review them.

We consider a volume that is bounded by walls and filled with a fluid--liquid or gas. In the real world, these would be a room or a building; in the similarity solution it would be a small-scale model of the room or building. Quantities pertaining to the walls will be given a subscript "w" and those pertaining to the fluid an "f". There are two length scales in such a system (see Fig. 2.1):

1. L_f which characterizes the size of the interior volume and determines the fluid motions.
2. L_w which characterizes the thickness of the walls and plays a role in conductive energy transport.

(The introduction of these two lengths should not be taken to imply that we are treating a simple cubic volume having uniform walls. The geometry of the full-scale system can be arbitrarily complex with all volume-determining lengths taken equal to scale-invariant constants times L_f and all wall

thickness-determining lengths equal to scale-invariant constants times L_w.)
There are two characteristic temperatures:

3. T_o, the average temperature,
4. ΔT, the amplitude of the temperature variation about T_o.

With a gas as a fluid medium the pressure becomes an important parameter:

5. P, the pressure.

There are three material properties of the fluid:

6. ν_f, the kinematic viscosity of the fluid,
7. α_f, the thermal diffusivity of the fluid,
8. k_f, the thermal conductivity of the fluid.

There are also two material properties of the walls:

9. α_w, the thermal diffusivity of the wall,
10. k_w, the thermal conductivity of the wall.

Thus, there is a total of 10 parameters. We have chosen to list thermal diffusivities rather than heat capacities per unit volume, ρc_p, where ρ is the mass density and c_p is the specific heat. The relationship between them is

$$\alpha = \frac{k}{\rho c_p} \quad . \tag{2.1}$$

At certain points it will be more convenient to use ρc_p rather than α as a parameter. No assumption about homogeneity of the walls is made by choosing these parameters, for it is assumed that all these internal characteristics will be scaled in the same way as the parameters listed above (see Appendix A).

We now turn to the equations of energy transport and derive a set of relations between the parameters of the real-world solution and those of the similarity solution. We will assume that the fluid medium is a gas which is not too dense so that we can use the properties of an ideal gas. We treat energy transport by conduction in the walls, by radiation, and by conduction and convection in the fluid, in that order.

The details of heat conduction in the walls are presented in Appendix A (also see Ref. 6). There we show that a wall is characterized by a derived time-scale $\tau_w = L_w C_w / U_w$ (where $L_w C_w$ is the heat capacity per unit area of the wall and U_w is the U-value of the wall, i.e., k_w/L_w for a uniform wall), a length scale L_w (where L_w is the thickness of the wall), and a dimensionless parameter $k_f L_w / k_w L_f$ which relates the heat fluxes in the fluid and the wall at their interface. In addition, for strict three-dimensional scaling of the heat conduction, the value of L_w/L_f must be held fixed. This last requirement need not be satisfied if one approximates the heat flow in the walls as being one-dimensional as is done in numerical simulations. Thus, consideration of heat conduction in the walls introduces two scaling requirements:

1. Constant ratio of wall and fluid U-values

$$\frac{k_f L_w}{k_w L_f} = \text{constant} \quad . \tag{2.2}$$

2. Constant ratio of wall and fluid-length scales for strict three-dimensional scaling

$$\frac{L_w}{L_f} = \text{constant} \quad . \tag{2.3}$$

In addition, the walls introduce a characteristic time τ_w which must be compared to another characteristic time of the system in order to develop a scaling requirement.

Radiative transport of energy is treated in detail in Appendix B (also see Ref. 6). There we show that this mode of transport is characterized by the emittances of the surfaces of the walls, a set of geometrical factors, and the temperatures of the surfaces. For typical materials, the values of the emittances are close to one for radiation in the infrared. We therefore assume that they are unchanged by the scaling. The geometrical factors are dimensionless and scale-invariant. This leaves only the temperatures to be scaled. The net radiative flux from a given surface will be proportional to the difference in the fourth powers of typical temperatures. For small temperature differences, this becomes

$$\text{net radiative flux} \sim 4\varepsilon \sigma T_o^3 \Delta T \quad , \tag{2.4}$$

where ε is the emittance, $\sigma = 5.67 \times 10^{-8}$ w/m^2 K^4 is the Steffan-Boltzmann constant, T_o is the average temperature, and ΔT is a typical temperature difference. We obtain a scaling condition by requiring that the ratio of this flux to a typical conductive flux, $k_w/L_w \Delta T$, be held constant:

3. Constant ratio of radiative flux to conductive flux

$$\frac{\varepsilon \sigma T_o^3 L_w}{k_w} = \text{constant} \quad . \tag{2.5}$$

Energy transport in the fluid is treated in detail in Appendix C (see also Ref. 6). There we use the Navier-Stokes equation and the Boussinesq approximation to describe the fluid motion and the ideal gas equation of state to give the pressure in terms of the density and temperature. The resulting

equations are scale-invariant if the Prandtl number Pr and the Grashof number Gr are held fixed where

$$Pr \equiv \frac{\nu_f}{\alpha_f} \quad , \tag{2.6}$$

where ν_f is the kinematic viscosity of the fluid and

$$\alpha_f = \left[\frac{k}{\rho c_p}\right]_f$$

is the thermal diffusivity of the fluid, and

$$Gr \equiv g \frac{\Delta T}{T_o} \frac{L_f^3}{\nu_f^2} \quad , \tag{2.7}$$

where g is the acceleration of gravity, T_o is the average temperature, and ΔT is the amplitude of the fluctuating part of the temperature. The approximations made impose the additional requirements

$$\frac{Mg}{RT_o} L_f \ll 1 \quad , \tag{2.8}$$

and

$$\frac{\nu^2}{L_f^2 c_p \Delta T} \ll 1 \tag{2.9}$$

for their validity, where M is the mean molar mass and R is the gas constant. These numbers have the values 10^{-3} and 10^{-15} for air so that these conditions are easily satisfied. The boundary conditions on the velocity are scale-invariant, and those on the temperature have been discussed above, see (2.2) and (2.3). Thus, the scaling requirements imposed by the fluid motion are

$$4.\quad \mathrm{Pr} = \text{constant} \quad , \tag{2.10}$$

$$5.\quad \mathrm{Gr} = \text{constant} \quad , \tag{2.11}$$

in addition to the two weak conditions (2.8) and (2.9) above. For air, $\mathrm{Pr} \sim 0.7$, and in typical building environments $\mathrm{Gr} \sim 10^{10}$. This value of the Grashof number implies[6] that the convection will span both laminar and turbulent regimes and convective film coefficients will not have any simple dependence on the characteristic parameters.

The Prandtl number is equal to the ratio of the characteristic times for the diffusion of momentum and thermal energy in the fluid; holding Pr constant ensures that they maintain the same relation to each other. The walls provide a third characteristic time $\tau_w = L_w C_w / U_w$ which also must scale in the same way that τ_f scales. We therefore have the final scaling requirement

$$6.\quad \frac{\tau_w}{\tau_f} = \text{constant} \quad . \tag{2.12}$$

We will now rewrite and summarize the derived scaling requirements. Adopting the notation that a parameter with a prime on it refers to the small-scale model solution while one with no prime refers to the full-scale solution, the scaling requirements can be written as

$$1.\quad \left[\frac{k_f}{k'_f}\right]\left[\frac{k'_w}{k_w}\right]\left[\frac{L_w}{L'_w}\right]\left[\frac{L'_f}{L_f}\right] = 1 \quad , \tag{2.13}$$

$$2.\quad \left[\frac{L_w}{L'_w}\right]\left[\frac{L'_f}{L_f}\right] = 1 \quad , \tag{2.14}$$

3. $$\left[\frac{\varepsilon}{\varepsilon'}\right]\left[\frac{T_o}{T_o'}\right]^3\left[\frac{L_w}{L_w'}\right]\left[\frac{k_w'}{k_w}\right] = 1 \ , \qquad (2.15)$$

4. $$\left[\frac{\nu_f}{\nu_f'}\right]\left[\frac{\alpha_f'}{\alpha_f}\right] = 1 \ , \qquad (2.16)$$

5. $$\left[\frac{\Delta T}{\Delta T'}\right]\left[\frac{T_o'}{T_o}\right]\left[\frac{L_f}{L_f'}\right]^3\left[\frac{\nu_f'}{\nu_f}\right]^2 = 1 \ , \qquad (2.17)$$

6. $$\left[\frac{L_w}{L_w'}\right]^2\left[\frac{L_f'}{L_f}\right]^2\left[\frac{\nu_f}{\nu_f'}\right]\left[\frac{\alpha_w'}{\alpha_w}\right] = 1 \ . \qquad (2.18)$$

The second and fourth requirements in this list have special status since they are relatively weak conditions. The second one ensures that heat conduction will scale in the strict three-dimensional sense rather than an approximate one-dimensional scaling. However, since the approximation of one-dimensional heat conduction is believed to be fairly accurate, the performance of the model should be insensitive to violations of this condition. The fourth condition ensures that the Prandtl number of the fluid remains fixed. However, for gases, the Prandtl number depends essentially on the number of degrees of freedom per gas molecule that are thermally excited and has a very limited range of values ($\sim$0.7 to $\sim$1). Thus, if we confine our model to gases having diatomic molecules, then this condition will be automatically satisfied and, if we use monatomic or triatomic gases, it will be only weakly violated. Mixtures of gases can be made with the proper value of Pr.

The fluid transport coefficients in (2.13) - (2.18) depend upon the average temperature T_o but, in the Boussinesq approximation, not on the fluctuating part of the temperature ΔT; they also depend on the average pressure P_o. We use mean-free-path arguments, which are described in Appendix D, to obtain the following expressions:

$$\nu_f = \nu_s \left[\frac{T_o}{T_s}\right]^{3/2} \left[\frac{P_s}{P_o}\right] , \tag{2.19}$$

$$k_f = k_s \left[\frac{T_o}{T_s}\right]^{1/2} , \tag{2.20}$$

$$\alpha_f = \alpha_s \left[\frac{T_o}{T_s}\right]^{3/2} \left[\frac{P_s}{P_o}\right] , \tag{2.21}$$

where the subscript s refers to standard conditions such as STP. These expressions assume that the specific heat of the gas is independent of temperature. That is, no additional molecular degrees of freedom are thermalized as the temperature is raised. Substitution of (2.19) - (2.21) into (2.13) - (2.18) exhibits explicitly all the temperature and pressure dependence of the scaling relations.

Before proceeding, it is useful to define a set of dimensionless scaling variables. They are:

Two temperature scaling variables

$$\delta \equiv \Delta T'/\Delta T ,$$
$$t \equiv T_o'/T_o . \tag{2.22}$$

Two length scaling variables

$$l_w \equiv L_w'/L_w \ ,$$
$$l_f \equiv L_f'/L_f \ . \tag{2.23}$$

Three fluid-property scaling variables

$$n_s \equiv \nu_s'/\nu_s \ ,$$
$$a_s \equiv \alpha_s'/\alpha_s \ , \tag{2.24}$$
$$\kappa_s \equiv k_s'/k_s \ .$$

Two wall-property scaling variables

$$a_w \equiv \alpha_w'/\alpha_w \ ,$$
$$\kappa_w \equiv k_w'/k_w \ . \tag{2.25}$$

One pressure scaling variable

$$p \equiv P_o'/P_o \ . \tag{2.26}$$

Thus, there is a total of ten scaling variables since we have assumed that the emittances are unchanged in scaling.

We substitute the expressions for the transport coefficients (2.19) - (2.21) into the scaling relations (2.13) - (2.18) and write them in terms of the scaling variables (2.22) - (2.26) to obtain

$$1. \quad t^{1/2} l_f^{-1} l_w \kappa_s \kappa_w^{-1} = 1 \ , \tag{2.27}$$

$$2. \quad l_f l_w^{-1} = 1 \ , \tag{2.28}$$

$$3. \quad t^3 l_w \kappa_w^{-1} = 1 \ , \tag{2.29}$$

$$4. \quad a_s n_s^{-1} = 1 \ , \tag{2.30}$$

$$5. \quad t^4 \delta^{-1} p^{-2} l_f^{-3} n_s^2 = 1 \ , \tag{2.31}$$

$$6. \quad t^{3/2} p^{-1} l_f^{-2} l_w^2 a_w^{-1} n_s = 1 \ . \tag{2.32}$$

These are the desired scaling relations--six conditions on ten parameters. This leaves much freedom to search for a practical implementation of the relations, which is the subject of the next section.

Before closing this section, however, we briefly discuss the scaling of heat sources. In particular, we consider how the solar flux, a point source of heat, and the infiltration of air scale. The solar flux S is energy per unit time and area. The relevant energy is the heat capacity of the system times the change in temperature. The heat capacity, which for simplicity is assumed to be all in the walls, is $C_w L_f^2 L_w$ and the temperature change is ΔT. The unit of time scales as τ_w and the unit of area is proportional to L_f^2. We then have

$$S \sim \frac{C_w L_f^2 L_w \Delta T}{\tau_w L_f^2} = \frac{k_w}{L_w} \Delta T \ . \tag{2.33}$$

This last form is just $U_w \Delta T$ which shows that the solar flux must scale in the same way as the conductive flux in the wall. We define the solar-flux variable as

$$\sigma = S'/S \quad , \tag{2.34}$$

and then

$$\sigma = \delta \kappa_w l_w^{-1} = \delta t^3 \quad , \tag{2.35}$$

where we have used a result from the next section, (3.9), to express σ in terms of temperature variables. The heat rate H for a point-source heater in the room will scale as $L_f^2 S$ and therefore, if $\eta \equiv H'/H$, then

$$\eta = \delta \kappa_w l_w^{-1} l_f^2 = \delta t^3 l_f^2 \quad . \tag{2.36}$$

Infiltration rates must also be scaled. For thermal modeling, infiltration can be thought of as a heat source (or sink) delivering heat at a rate equal to the heat capacity per unit volume of the fluid $(\rho c_p)_f$, times the volume of the fluid L_f^3, times the inside-to-outside temperature difference $\sim \Delta T$, times the rate of infiltration in fluid-volume changes per unit time $\dot{N}$. The ratio of these heat rates for full- and small-scale models is then $\gamma_f l_f^3 \delta \dot{n}$, where $\dot{n} = \dot{N}'/\dot{N}$. Equating this to the last form of (2.36) yields

$$\dot{n} = t^3 l_f^{-1} \gamma_f^{-1} \quad , \tag{2.37}$$

(see (3.7) for γ) for the scaling of infiltration rates.

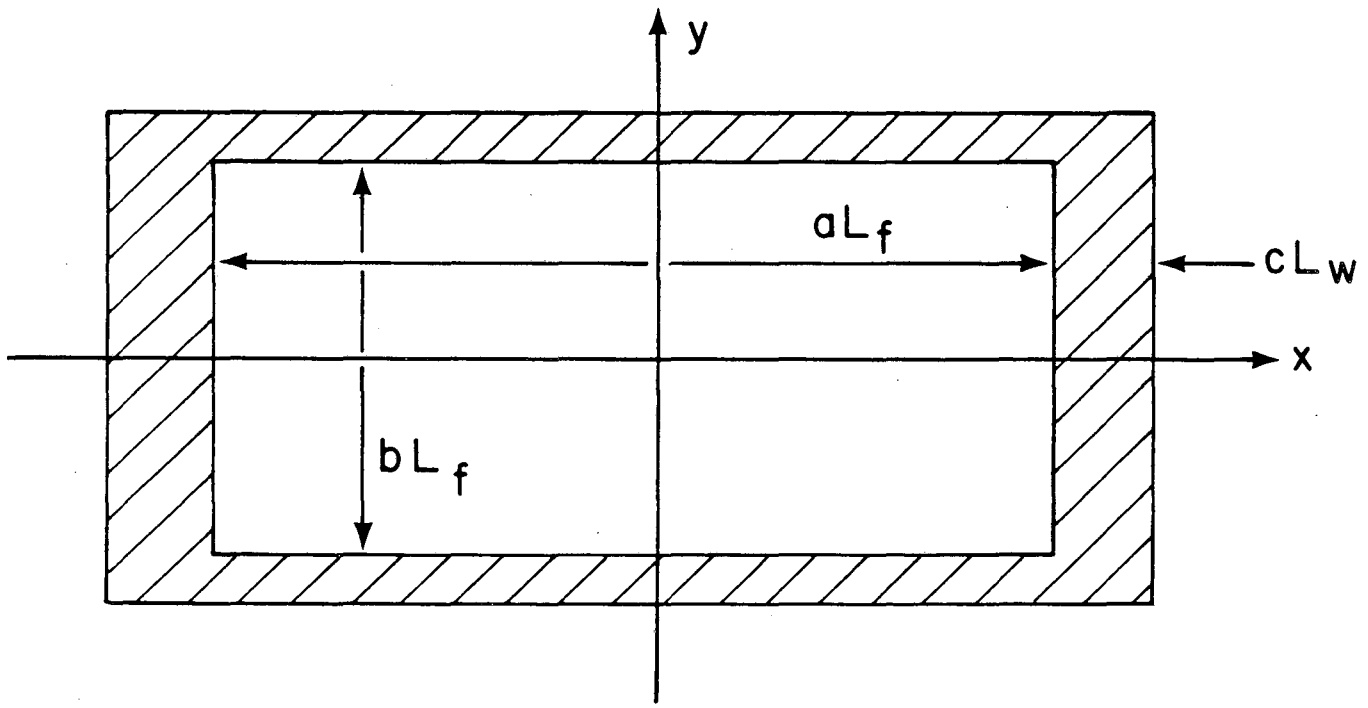

XBL 8110-1453

Fig. 2.1. Cross section through a typical room. The constants, a, b, c, ... are scale invariant numbers which define the geometry of the room.

3. Implementation of the Scaling Relations

We have already noted that the second and fourth scaling relations, (2.28) and (2.30), have special status. The second one is relatively unimportant and the fourth one is relatively easy to satisfy. Therefore, throughout this section, we assume that (2.30) is satisfied and use it to eliminate the parameter n_s in favor of a_s. In the first part of this section, we also assume that (2.28) has been relaxed and we can scale fluid and wall lengths independently. Later in the section, we will consider the implications of (2.28). Our method involves rewriting the scaling relations in forms that reveal the material properties needed to achieve practical scaling and then substitute the values of specific material properties to see how much scaling can be accomplished with available materials.

Our discussion is facilitated by the introduction of one more parameter and the relation that defines it. The parameter is the ratio of a characteristic time of the model to that of the real-world model. We take the ratio of the wall times and define

$$7. \qquad \tau \equiv \tau_w'/\tau_w = l_w^2\, a_w^{-1} \quad . \tag{3.1}$$

This parameter is important from a practical point of view since τ^{-1} will indicate how much faster the small-scale model performs as compared to the full-scale system.

The scaling relations are rather complex and the constraints that they impose are most easily visualized if they are written in several forms. In this first discussion, we relax the second relation, $l_f = l_w$, and eliminate n_s using the fourth relation, $n_s = a_s$. There are ten remaining variables, including τ, and five relations, including (3.1). One must then make a choice of dependent and independent variables. The variables δ, t, p,

l_f, and l_w are a natural choice for dependent variables since they are arbitrarily (within limits) and independently adjustable by the modeler. The values of the variables a_s, κ_s, a_w, and κ_w are constrained by the materials available and therefore are a natural choice for independent variables. For a start, we also choose τ as an independent variable since it would be nice to be able to specify the data rate for the model. With this choice of variables, Eqs. (2.27), (2.29), (2.31), (2.32), and (3.1) become

$$7. \qquad l_w = \tau^{1/2} (a_w \kappa_w^{-2})^{1/2} \kappa_w \ , \tag{3.2}$$

$$1. \qquad l_f = \tau^{5/12} (a_w \kappa_w^{-2})^{5/12} \kappa_s \ , \tag{3.3}$$

$$6. \qquad p = \tau^{-1/12} (a_w \kappa_w^{-2})^{-13/12} (a_s \kappa_s^{-2}) \ , \tag{3.4}$$

$$3. \qquad t = \tau^{-1/6} (a_w \kappa_w^{-2})^{-1/6} \ , \tag{3.5}$$

$$5. \qquad \delta = \tau^{-7/4} (a_w \kappa_w^{-2})^{1/4} \kappa_s \ , \tag{3.6}$$

When written in this from, the equations show the important role played by the combination of parameters $(a\ \kappa^{-2})$ for the fluid or the wall. We write this combination in a more palpable form by introducing the ratio of heat capacities per unit volume

$$\gamma = \rho' c_p' / \rho c_p \tag{3.7}$$

for the fluid or the wall. We then have $(a\kappa^{-2}) = (\gamma\kappa)^{-1}$. The second important point that these equations make is that l_f and l_w obey curiously different scaling laws. This difference provided the motivation for relaxing the second scaling relation, $l_f = l_w$, in this first discussion.

Further progress in understanding these equations can be made by using (3.5) to eliminate $a_W \kappa_W^{-2} = (\gamma_W \kappa_W)^{-1}$ in favor of t. This choice is motivated by practical considerations that restrict the range of t to roughly $1 \leq t < 2$, while $\gamma_W \kappa_W$ is less severely restricted. We then have

3. $$\gamma_W \kappa_W = \tau t^6 \quad , \tag{3.8}$$

7. $$l_W = t^{-3} \kappa_W \quad , \tag{3.9}$$

1. $$l_f = t^{-5/2} \kappa_s \quad , \tag{3.10}$$

6. $$p = \tau t^{13/2} (\gamma_s \kappa_s)^{-1} \quad , \tag{3.11}$$

5. $$\delta = \tau^{-2} t^{-3/2} \kappa_s \quad . \tag{3.12}$$

The last two equations suggest which gas properties one should look for. We hope that τ is a small number. Therefore, since δ is proportional to τ^{-2} in (3.12) which is large, we want a small κ_s to keep δ to a reasonable value. At the same time we don't want $\gamma_s \kappa_s$ to be small since then p would be large. Thus, we want a gas that has a small thermal conductivity and a large heat capacity per unit volume. Such a gas is uncommon because thermal conductivity is proportional to heat capacity. We should be looking for a gas having massive molecules with large collision cross sections which would suppress its transport properties (see Appendix D). This kind of compromise between p and δ is exemplified by the numbers given in Table 3.1. There, we list the values of p and δ for the noble gases with the choice $\tau = 1/24$ and $t = 2$. We see that p is an increasing function of atomic number while δ is a decreasing function.

As a final form of the relations, we change the status of τ to that of a dependent variable and p to an independent one using (3.11). We then have

6. $$\tau = \gamma_s \kappa_s p\, t^{-13/2} \quad , \tag{3.13}$$

5. $$\delta = \gamma_s^{-2} \kappa_s^{-1} p^{-2} t^{23/2} \quad , \tag{3.14}$$

3. $$\gamma_w \kappa_w = p\, t^{-1/2} \gamma_s \kappa_s \quad . \tag{3.15}$$

These equations emphasize the antagonistic nature of the requirements of small τ and not too large δ. One promising possibility is that of working at room temperature and pressure, p = t = 1. We specialize the equations to this case and give the numbers resulting from choosing Xe as the gas:

$$\tau = \gamma_s \kappa_s = 0.15\ (\text{Xe}) \quad , \tag{3.16}$$

$$\delta = \gamma_s^{-2} \kappa_s^{-1} = 9.4\ (\text{Xe}) \quad , \tag{3.17}$$

$$\gamma_w \kappa_w = \gamma_s \kappa_s = 0.15\ (\text{Xe}) \quad , \tag{3.18}$$

$$l_w = \kappa_w = ?\ (\text{Xe}) \quad , \tag{3.19}$$

$$l_f = \kappa_s = 0.21\ (\text{Xe}) \quad . \tag{3.20}$$

This gives a factor of 6.6 speed up, a 4.6-fold reduction in L_f, and a scaling of L_w that is unspecified.

The fact that l_w is not specified in the above example suggests that it may be easy to satisfy the second scaling condition, $l_f = l_w$, which we have ignored up to now. Equating (3.9) and (3.10) shows that this condition will be satisfied if

$$\kappa_w = t^{1/2} \kappa_s \quad . \tag{3.21}$$

However, this may be difficult to achieve in practice because we seek a gas having small κ_s and $t^{1/2}$ cannot be large. Thus, (3.21) implies that we use materials having small κ_w, $\kappa_w = 0.21$ and $\gamma_w = 0.70$ in the above example, and such materials may not exist. Nevertheless, full three-dimensional similarity is sufficiently important, both in the context of the above discussion, and in the broader context of a volume made up of several rooms having interior walls and doorways, that a search for such materials should be made.

We conclude this section by presenting our scaling relations in their most useful form and giving some more examples. We write the scaled parameters in terms of fluid parameters and pressure and temperature on the assumption that wall parameters can be adjusted by making composite walls. We then have the wall parameters given by

$$\kappa_w = \kappa_s t^{1/2} , \tag{3.22}$$

$$\gamma_w = \gamma_s p\, t^{-1} , \tag{3.23}$$

the length scaling with $l_w = l_f = 1$ and

$$1 = \kappa_s\, t^{-5/2} , \tag{3.24}$$

$$\delta = \gamma_s^{-2}\, \kappa_s^{-1}\, p^{-2}\, t^{23/2} , \tag{3.25}$$

and the time scale

$$\tau = \gamma_s\, \kappa_s\, p\, t^{-13/2} . \tag{3.26}$$

The values of the coefficients in these equations are given in Table 3.2 for the following choices of gases: SF_6, SO_2, Ar, Xe. Note that these numbers are much more uncertain than the two significant figures given. For example, the values of the thermal conductivity of air at 0 °C given in Refs. 9, 11, and 12 rounded off to two significant figures are 24, 25, and 23 x 10^{-3} w/m K respectively. Nevertheless, one can see that these four gases span a large range of possibilities. In order to emphasize this point, in Table 3.3 we present the values of l, δ and τ for these four gases for $p = 1$ or 10 and $t = 1$ or 2. In practice, tables such as this should be searched for small values of l and τ that are associated with not-too-large values of δ, e.g., $\delta < 10$. Thus, SF_6 with $p = 10$ and $t = 2$ looks like good possibility. However, SF_6 has an infrared vibrational band at 347 cm^{-1} which is at an energy equivalent to 516K. Thus, the requirement that the gas in the scale model be optically thin to the predominant thermal radiation probably imposes the requirement that $t < 1.5$ for SF_6. Nevertheless, SF_6 is a good candidate and any competing gas must pass all the tests presented in the preceeding discussion.

Table 3.1. Values of p and δ for the noble gases calculated from Eqs. (3.11) and (3.12) with $\tau = 1/24$ and $t = 2$.

Gas	He	Ne	Ar	Kr	Xe
p	0.245	2.84	7.81	14.6	25.3
δ	1170	381	139	74.1	42.8

Table 3.2. Values of the coefficients in Eqs. (3.22) - (3.26) for several gases.

Gas	κ_s	γ_s	$\gamma_s^{-2}\kappa_s^{-1}$	$\gamma_s\kappa_s$
SF_6[10]	0.55	3.3	0.17	1.8
SO_2[9]	0.36	1.4	1.4	0.50
Ar[11]	0.68	0.70	3.0	0.48
Xe[11]	0.21	0.70	9.7	0.15

Table 3.3. Values of l, δ, and τ derived from Eqs. (3.22) - (3.26).

Gas	p	t	l	δ	τ
SF_6	1	1	0.55	0.17	1.8
	10	1	0.55	0.0017	18
	1	2	0.10	497	0.020
	10	2	0.10	4.97	0.20
SO_2	1	1	0.36	1.4	0.51
	10	1	0.36	0.014	5.1
	1	2	0.064	4,100	0.0056
	10	2	0.064	41	0.056
Ar	1	1	0.68	3.0	0.48
	10	1	0.68	0.030	4.8
	1	2	0.12	8,700	0.0053
	10	2	0.12	87	0.053
Xe	1	1	0.21	9.4	0.15
	10	1	0.21	0.094	1.5
	1	2	0.038	27,000	0.0017
	10	2	0.038	270	0.017

4. Conclusion

We have derived a set of six scaling conditions on the ten scaling variables that characterize a scale-model building. These conditions, based upon spatial and temporal scaling, allow a rich variety of possibilities which have not yet been fully explored. We discuss below three areas that need further study: (1) the use of gas mixtures; (2) the proper wall materials; and (3) the validity of the Boussinesq approximation used to describe free convection.

The use of a mixture of gases for an atmosphere may allow additional freedom in meeting the requirements of scaling. The desirable properties of such a mixture are: (a) the Prandtl number must be the same as that of air (0.72); (b) the thermal conductivity should be low and the heat capacity per unit volume high for proper scaling; and (c) the gases should not have any absorption bands in the infrared as they would impede radiative transport.

In order to have full three-dimensional scaling, the walls of the scale model must be made of materials of moderate heat capacity per unit volume and low thermal conductivity. These goals may be achieved by a combination of good design and the use of exotic materials. However, this is an area for future study. See Appendix E for one solution to this problem.

The validity of the Boussinesq approximation in studies of free convection is taken more or less as an article of faith. A quantitative justification of its use in this particular context would place this study on firmer ground. This is a question for which there is already a large literature.

Acknowledgements

In the early phases of this work, we benefited from discussions with Allan M. Portis. The support and encouragement of John Brogan is also gratefully acknowledged. This work was supported by the Assistant Secretary for Conservation and Renewable Energy, Office of Buildings and Community Systems, Buildings Division of the U.S. Department of Energy under Contract DE-AC03-76SF00098.

Appendix A. Energy Transport by Conduction in Walls

The sole mechanism of energy transport through the solid walls of a building is conduction. There is also transport by conduction in the fluid medium but there it plays a secondary role to convective transport. In this appendix we consider conductive transport in the walls.

The conduction of heat is described by the heat equation (see Ref. 6).

$$\rho c_p \frac{\partial T_w}{\partial t} = \vec{\nabla} \cdot [k \vec{\nabla} T_w] \quad , \tag{A.1}$$

where ρ is the mass density, c_p the specific heat, and k the thermal conductivity of the wall, all of which may depend upon position in an inhomogeneous medium. The temperature distribution of the wall $T_w(r,t)$ is determined by (A.1) plus boundary and initial conditions. The transients that are excited by the initial conditions are of no interest since they die out quickly. Thus, we need only consider (A.1) plus boundary conditions. Note that (A.1) is just the statement of local conservation of thermal energy. For, $\rho\ c_p$ is the heat capacity per unit volume and therefore the left-hand side of (A.1) is the time-derivative of thermal energy density $\rho\ c_p\ T_w$. The right-hand side is minus the divergence of the thermal energy current $-k \vec{\nabla} T_w$.

We assume that a given wall can be represented by N layers having constant properties. Eq. (A.1) for the i^{th} layer then becomes

$$(\rho c_p)_i \frac{\partial T_i}{\partial t} = k_i \nabla^2 T_i \quad , \tag{A.2}$$

and the boundary conditions become:

continuity of the temperature

$$T_i = T_{i+1} \tag{A.3}$$

and continuity of the current

$$k_i \, \hat{n} \cdot \vec{\nabla} T_i = k_{i+1} \, \hat{n} \cdot \vec{\nabla} T_{i+1} \quad , \tag{A.4}$$

at the interfaces between the layers. The unit vector $\hat{n}$ is the normal to the interface in (A.4). We can include the external boundary conditions if we interpret i = 0 or N+1 to be the fluid f in (A.3) and (A.4). For the discussion of this appendix, the fluid temperature T_f is assumed to be given.

We denote the thickness of the i^{th} layer by L_i and define the total thickness of the wall

$$L_w \equiv \sum_{i=1}^{N} L_i \quad , \tag{A.5}$$

the average heat capacity per unit volume

$$C_w \equiv \frac{1}{L_w} \sum_{i=1}^{N} (\rho \, c_p)_i \, L_i \quad , \tag{A.6}$$

and the effective static thermal resistance

$$\frac{L_w}{k_w} = \sum_{i=1}^{N} \frac{L_i}{k_i} \quad .$$

The static properties of the wall are completely determined by L_w and k_w. The dynamic properties will also depend upon C_w and the dimensionless internal parameters L_i/L_w, $(\rho \, c_p)_i/C_w$, and k_i/k_w. In our search for similarity solutions, we assume that these dimensionless internal parameters are fixed and we vary L_w, C_w, and k_w. This may be easier to do on paper than in practice.

We now rewrite Eqs. (A.2) - (A.4) in a form appropriate for scaling. Since temperature carries its own dimensions, there is nothing to be gained by rescaling it. We choose L_w as our unit of length, $\vec{r}_w \equiv \vec{r}/L_w$, $\vec{\nabla}_w \equiv L_w \vec{\nabla}$, and write (A.2) as

$$\tau_w \frac{(\rho c_p)_i}{C_w} \frac{\partial T_i}{\partial t} = \frac{k_i}{k_w} \nabla_w^2 T_i \quad , \tag{A.8}$$

where we have introduced the characteristic time of the wall

$$\tau_w \equiv \frac{L_w^2}{\alpha_w} \quad , \tag{A.9}$$

and the effective thermal diffusivity of the wall

$$\alpha_w \equiv \frac{k_w}{C_w} \quad , \tag{A.10}$$

which is strictly a material property. Eqs. (A.3) are unchanged and, for i=1, ..., N-1, Eqs. (A.4) become

$$\left[\frac{k_i}{k_w}\right] \hat{n} \cdot \vec{\nabla}_w T_i = \left[\frac{k_{i+1}}{k_w}\right] \hat{n} \cdot \vec{\nabla}_w T_{i+1} \quad . \tag{A.11}$$

For i = 0 or N, Eqs. (A.3) and (A.4) involve an interface between the wall and the fluid. For example, setting i = 0, we have $T_f \equiv T_0 = T_1$ and

$$k_f \hat{n} \cdot \vec{\nabla} T_f = k_1 \hat{n} \cdot \vec{\nabla} T_1 \quad . \tag{A.12}$$

We assume that the fluid volume has a characteristic length L_f so that $\vec{r}_f = \vec{r}/L_f$ and $\vec{\nabla}_f = L_f \vec{\nabla}$. Equation (A.12) then becomes

$$\left[\frac{k_f}{k_w}\right] \frac{1}{L_f} \hat{n} \cdot \vec{\nabla}_f T_f = \left[\frac{k_i}{k_w}\right] \frac{1}{L_w} \hat{n} \cdot \vec{\nabla}_w T_1 \quad . \tag{A.13}$$

A similar expression is obtained for i = N.

Apart from the internal wall parameters that are assumed to be held constant during scaling, the above equations involve the characteristic time for the wall τ_w (A.9) and the parameter $k_f L_w / k_w L_f$ in (A.13), both of which may change during scaling. These are the only scaling variables if one assumes, as in numerical simulations, that the heat conduction is one-dimensional in the direction perpendicular to the wall surface. If one requires exact three-dimensional scaling, then the ratio L_w/L_f is also a scaling variable. This variable enters through the specification of the boundary conditions such as (A.13). This is best demonstrated by an example. Consider a square wall surface of dimensions $L_f \times L_f$ which crosses the x-axis at the point $x = L_f/2$ and is oriented perpendicular to the x-axis. The surface is the set of points satisfying: $x = L_f/2$, $L_f/2 < y$, $z < L_f/2$. If we translate these conditions into conditions on $\vec{r}_f$, the argument of T_f in (A.13), we have: $x_f = 1/2$, $-1/2 < y_f, z_f < 1/2$. This is independent of scale. However, if we translate these conditions into conditions on $\vec{r}_w$, the argument of T_1 in (A.13), we have:

$$x_w = \frac{L_f}{2L_w} \quad , \quad -\frac{L_f}{2L_w} < y_w \quad , \quad z_w < \frac{L_f}{2L_w}$$

which is not independent of scale unless we hold L_w/L_f fixed during the scaling. The condition $x_w = L_f/2L_w$ does not break the scaling since it can be removed by a translation of coordinates. Thus, L_w/L_f only enters in the transverse y- and z- directions and holding it constant is necessary for exact three-dimensional scaling. However, if we assume that the heat conduction is one-dimensional, then the temperatures in (A.13) are independent of y and z, and L_w/L_f can be varied without violating scaling requirements.

We argue that the condition L_w/L_f = constant is a relatively unimportant scaling condition. This condition ensures that transverse heat conduction scales properly. However, if transverse heat conduction is a 10% effect, then we will not make large errors if this condition is violated.

Appendix B. Energy Transport by Radiation

We assume that the walls of the enclosure radiate as gray bodies. They radiate energy as

$$E = \varepsilon \sigma T^4 \quad , \tag{B.1}$$

where E is the total power radiated per unit area, the emittance ε is about one for typical materials radiating in the infrared, and $\sigma = 5.67 \times 10^{-8}$ $w/m^2\ k^4$ is the Stefan-Boltzmann constant. We also assume that the fluid medium is transparent so that radiation transports energy from and to the interior surfaces only. The power radiated from an element of area d^2r_1 of surface 1 and incident upon an element of area d^2r_2 of surface 2 is given by (See Ref. 6)

$$dP_{1\to 2} = \frac{E_1}{\pi} \frac{(\hat{n}_1 \cdot \vec{r}_{12})\ (\hat{n}_2 \cdot \vec{r}_{21})}{r_{12}^4}\ d^2r_1\ d^2r_2 \quad , \tag{B.2}$$

where E_1 is given by (B.1) for surface 1, $\hat{n}_1$ and $\hat{n}_2$ are the inward-pointing normals of the two surfaces, $\vec{r}_{ij} = \vec{r}_i - \vec{r}_j$ is the vector from point $\vec{r}_j$ on surface j to point $\vec{r}_i$ on surface i.

In addition to radiating energy, the surfaces will also reflect it. The power leaving surface i per unit area will be

$$J_i = (1 - \varepsilon_i)\ G_i + \varepsilon_i \sigma T_i^4 \quad , \tag{B.3}$$

where G_i is the incident flux of radiant energy and we have used the gray-body assumption to write the reflectance of the i^{th} surface as $1-\varepsilon_1$.

The geometry of the system is simplified if we assume that all surfaces are flat. We then obtain the incident fluxes G_i from the set of equations

$$G_i = \sum_{j \neq 1} F_{ij} J_j \quad , \tag{B.4}$$

where the F_{ij} are geometrical factors obtained from (B.2)

$$F_{ij} = \frac{1}{\pi} \int \frac{(\hat{n}_1 \cdot \vec{r}_{ij})\ (\hat{n}_j \cdot \vec{r}_{ji})}{r_{ij}^4} \ d^2 r_j \quad . \tag{B.5}$$

This treatment assumes that the surfaces chosen are small enough so that each one has a constant temperature and radiative environment. Substitution of (B.4) and (B.3) yields a set of equations for the radiosities J_i.

The net rate of energy loss from surface i is the difference between what goes out and what comes in,

$$J_i - G_i = G_i[\sigma T_i^4 - G_i] \quad .$$

The parameters that figure in the above discussion are the emittances ε_i, the geometrical factors F_{ij}, and the temperatures T_i. We assume that the emittances are not changed by the scaling since they are close to one for most materials radiating in the infrared. The geometrical factors are dimensionless and scale-invariant by definition. The temperatures are the only variables that can be changed by scaling.

The solution of Eqs. (B.3) and (B.4) will yield net fluxes that are proportional to differences in the fourth power of temperature or, assuming small temperature differences, we have

$$\text{net radiative flux} \sim 4\ \varepsilon\ \sigma\ T_0^3\ \Delta T \quad , \tag{B.6}$$

where T_0 is the average temperature and ΔT is a typical temperature difference. For scaling, this flux must be compared to other fluxes of energy.

Appendix C. Energy Transport by Conduction and Convection in the Fluid

The fluid motions are described in the hydrodynamic approximation of the Navier-Stokes equations (see Ref. 6). This approximation is valid as long as the fluid properties change insignificantly over a molecular mean-free-path ($\tilde{<}$ one micron for a gas at standard conditions) and during a molecular mean-free-time ($\tilde{<}$ 10^{-9} sec for a gas at standard conditions). These conditions are well satisfied in the situations that we are concerned with. A further approximation to these equations--the Boussinesq approximation[7]--is used to describe free convection. This approximation can be crudely described as one that takes buoyancy forces into account only to leading order. The validity of this approximation is hard to quantify. In practice, however, it has proven to be a useful guide in studies of convection, and we will assume that it is a satisfactory representation of our system.

The equations resulting from these approximations are written in a dimensionless, scale-invariant form which involves certain dimensionless groups of parameters such as the Prandtl number and the Grashof number. These numbers must be held constant during scaling so that dynamic similarity is maintained; this requirement imposes scaling conditions on the parameters.

The Navier-Stokes equations are statements of local conservation of mass, momentum, and energy. The state of the fluid is described by the mass density ρ, the velocity $\vec{v}$, and the temperature T which are all functions of position $\vec{r}$ and time t. Conservation of mass is expressed by the continuity equation

$$\frac{\partial \rho}{\partial t} + \vec{\nabla} \cdot (\rho \vec{v}) = 0 \quad . \tag{C.1}$$

Conservation of momentum is expressed by

$$\rho \left[\frac{\partial \vec{v}}{\partial t} + (\vec{v} \cdot \vec{\nabla})\vec{v}\right] = -\vec{\nabla}P + \rho\vec{g} + \mu\nabla^2\vec{v} + \left(\zeta + \frac{\mu}{3}\right)\vec{\nabla}(\vec{\nabla}\cdot\vec{v}) \quad , \qquad (C.2)$$

where P is the pressure, $\vec{g}$ is the gravitational acceleration, and μ and ζ are viscosities. This equation is a disguised version of the statement: time derivative of the momentum density plus divergence of the momentum current equals zero. The final conservation of energy equation is

$$\rho c_p \left[\frac{\partial T}{\partial t} + (\vec{v} \cdot \vec{\nabla})T\right] = k\nabla^2 T + \mu \left[\nabla_\alpha v_\beta + \nabla_\beta v_\alpha\right] \nabla_\alpha v_\beta$$

$$+ \left(\zeta - \frac{2\mu}{3}\right) (\vec{\nabla} \cdot \vec{v})^2 \quad ,$$

where c_p is the specific heat and k is thermal conductivity of the fluid (we suppress the subscript "f" in this appendix whenever our meaning is unambiguous.). The left-hand side plus the first term on the right-hand side describe convective and conductive transport of thermal energy. The remaining two terms on the right-hand side describe the dissipation of fluid kinetic energy into thermal energy. In the first of these latter two terms, the indices α and β are summed over the three components of the respective vectors. Equations (C.1) - (C.3) are five equations in the five unknowns--ρ, $\vec{v}$, and T plus the additional variable--the pressure P. They are completed by an equation of state for the fluid: $P = P(\rho,T)$. We will use the ideal gas equation of state

$$P = \frac{R}{M}\rho T \quad , \qquad (C.4)$$

for the systems we treat. Here, R is the gas constant and M is the mean molar mass of the gas. The transport coefficients are discussed in Appendix D.

These equations must be supplemented by boundary conditions. The appropriate ones for free convection in an enclosed volume are

$$\vec{v} = 0 \quad , \tag{C.5}$$

$$T_f = T_1 \quad , \tag{C.6}$$

$$k_f \, \hat{n} \cdot \vec{\nabla} T_f = k_1 \, \hat{n} \cdot \nabla T_1 \quad , \tag{C.7}$$

at the surfaces. Here, T_1 is the temperature of the innermost surface of the wall, k_1 its thermal conductivity, and $\hat{n}$ its unit normal (see Eq. (A.12)). The first of these is the standard no-slip boundary condition of viscous hydrodynamics. The last two impose continuity of temperature and heat flux at the surfaces.

We first consider the static isothermal solution to Eqs. (C.1) - (C.7). This is given by

$$\rho = \rho_0(z) \quad , \quad T = T_0 \quad , \quad \vec{v} = 0 \quad , \tag{C.8}$$

where z is taken in the vertical direction and

$$\rho_0(z) = \rho_0^0 \exp \left(- \frac{Mg}{RT_0} z\right) \quad , \tag{C.9}$$

with ρ_0^0 equal to the constant density of the gas at the floor z = 0. The scale height of the atmosphere RT_0/Mg has the approximate value of 8 km for air at standard temperature. Thus for most purposes, ρ_0 can be treated as a constant over distances less than tens of meters; quantitatively, ρ_0 can be treated as a constant if

$$\frac{Mg}{RT_0} L_f \ll 1 \quad , \tag{C.10}$$

where L_f is the characteristic length scale of the fluid volume.

In order to estimate the magnitudes of the various terms in the Navier-Stokes equations and to write them in a scale-invariant form, we consider the various units we can form from the constants that appear in them. We have already introduced a unit of length L_f -- the characteristic size of the fluid volume. We have two choices for a unit of time

$$\tau_f = \frac{L_f^2}{\nu} \quad \text{or} \quad \tau_f' = \frac{L_f^2}{\alpha} \quad , \text{ where } \quad \nu = \frac{\mu}{\rho}$$

is the kinematic viscosity (or better--the momentum diffusivity) and $\alpha = k/\rho c_p$ is the thermal diffusivity. The ratio of these two time scales is the Prandtl number

$$Pr \equiv \frac{\nu}{\alpha} \quad . \tag{C.11}$$

For most gases Pr ranges between 0.7 and 1, and there is no reason to choose one time scale over the other--we choose τ_f as our unit of time. However, for dynamic similarity we must require that momentum and heat diffuse with equal relative rapidity, which leads to the scaling requirement: Pr = constant. With these units of length and time, we have ν/L_f as our unit of speed. We will use ρ_0 as a weakly variable unit of density. In spite of the fact that these are "natural" units, they turn out to have values that are not well suited for the problem at hand. If we consider air at STP, then $\nu = 1.5 \times 10^{-5}$ m^2/s and, if we take $L_f = 5$ m, then $\tau_f = 460$ hours and the unit of velocity is $\nu/L_f = 3 \times 10^{-6}$ m/sec. Thus, in these units, we can expect dimensionless times to be small and dimensionless velocities to be large. For air, the density is given by $\rho_0^0 = 1.3$ kg/m^3.

We write the density and velocity in the system of units just described as

$$\rho(\vec{r},t) = \rho_0(L_f z_f)\ \tilde{\rho}\ (\vec{r}_f,t_f) \quad , \tag{C.12}$$

$$\vec{v}(r,t) = \frac{\nu}{L_f}\ \tilde{\vec{v}}\ (\vec{r}_f,\ t_f) \quad , \tag{C.13}$$

where ρ_0 is given by (C.9) and

$$\vec{r}_f = \frac{\vec{r}}{L_f} \quad , \quad t_f = \frac{t}{\tau_f} \quad . \tag{C.14}$$

In addition, we write the temperature as

$$T(\vec{r},t) = T_0 + \Delta T\ \tilde{T}\ (\vec{r}_f,\ t_f) \quad , \tag{C.15}$$

where T_0 is the average temperature and ΔT is the amplitude of the fluctuating part of the temperature. Substituting these expressions into (C.1) - (C.3) and using the ideal gas equation of state (C.4) for the pressure yields the equations

$$\frac{\partial\tilde{\rho}}{\partial t_f} - \frac{Mg}{RT_0}\ L_f\tilde{v}_z + \vec{\nabla}_f \cdot (\tilde{\rho}\tilde{\vec{v}}) = 0 \quad , \tag{C.16}$$

where $\nabla_f = L_f\nabla$,

$$\frac{\partial\tilde{\vec{v}}}{\partial t_f} + (\vec{v}\cdot\vec{\nabla}_f)\ \tilde{\vec{v}} = Gr\ \tilde{T}\ \hat{z} - \frac{RT_0L_f^2}{M\nu^2}\left[\left(1 + \frac{\Delta T}{T_0}\ \tilde{T}\right)\frac{\vec{\nabla}_f\tilde{\rho}}{\tilde{\rho}} + \frac{\Delta T}{T_0}\ \vec{\nabla}_f\tilde{T}\right]$$

$$+ \nabla_f^2\ \tilde{\vec{v}} + \left(\frac{\zeta}{\mu} + \frac{1}{3}\right)\vec{\nabla}_f\ (\vec{\nabla}_f\cdot\tilde{\vec{v}}) \quad , \tag{C.17}$$

where we have defined the Grashof number as

$$Gr \equiv g \frac{\Delta T}{T_o} \frac{L_f^3}{\nu^2} , \tag{C.18}$$

with g the magnitude of the gravitational acceleration and $\hat{z}$ a unit vector in the vertical direction. For air at 300 K, we have

$$Gr \approx 10^{11} \left[\frac{\Delta T}{5^\circ C}\right] \left[\frac{L_f}{5m}\right]^3 ,$$

which indicates that the flow is in the transition region between laminar and turbulent, $10^9 < Gr < 10^{11}$. The temperature equation is

$$\frac{\partial \tilde{T}}{\partial t_f} + (\tilde{\vec{v}} \cdot \vec{\nabla}_f)\, \tilde{T} = \frac{\tilde{T}}{Pr} + \frac{\nu^2}{L_f^2 c_p \Delta T} (\nabla_{f\alpha} \tilde{v}_\beta + \nabla_{f\beta} \tilde{v}_\alpha)\, \nabla_{f\alpha} \tilde{v}_\beta + (\frac{\zeta}{\mu} - \frac{2}{3})\, (\vec{\nabla}_f \cdot \tilde{\vec{v}})^2 , \tag{C.19}$$

where the Prandtl number Pr was introduced in (C.11).

We now perform some drastic approximations to simplify the form of the equations. We first note that the second term in (C.16) is proportional to the small parameter $Mg/RT_o\, L_f$, (C.10), and we ignore it. The buoyancy forces have been taken into account in the term proportional to Gr in (C.17). Therefore, to lowest order, we can set $\tilde{\rho} = 1$ and (C.16) becomes

$$\vec{\nabla}_f \cdot \tilde{\vec{v}} = 0 , \tag{C.20}$$

or incompressible flow. All terms in (C.17) and (C.18) that are proportional to $\nabla_f^{\rightarrow}\cdot\tilde{\vec{v}}$ or $\vec{\nabla}_f\tilde{\rho}$ now can be dropped. The term in (C.17) proportional to $\vec{\nabla}_f\tilde{T}$ represents the acceleration of the gas due to its own thermal expansion. This is known to be a small effect, so this term is dropped. The dissipation term in (C.19) is multiplied by the constant $\nu^2/L_f^2 c_p \Delta T$ the value of which is 1.8×10^{-15} for air with $L_f = 5m$ and $\Delta T = 5°C$, so we drop this term. Equations (C.17) and (C.19) then become

$$\frac{\partial \tilde{\vec{v}}}{\partial t_f} + (\tilde{\vec{v}}\cdot\vec{\nabla}_f)\tilde{\vec{v}} = Gr\ \tilde{T}\hat{z} + \nabla_f^2\tilde{\vec{v}} \quad , \tag{C.21}$$

$$\frac{\partial \tilde{T}}{\partial t_f} + (\tilde{\vec{v}}\cdot\vec{\nabla}_f)\tilde{T} = \frac{1}{Pr}\nabla_f^2\tilde{T} \quad . \tag{C.22}$$

These equations are scale-invariant if Gr and Pr are held fixed and the approximations (C.10) and

$$\frac{\nu^2}{L_f^2 c_p \Delta T} \ll 1 \quad , \tag{C.23}$$

remain valid. These approximations are easily satisfied.

The boundary condition on the velocity (C.5) is independent of scale. The boundary conditions on the temperature (C.6) and (C.7) have been discussed in Appendix A, see Eq. (A.12).

Appendix D. Mean-Free-Path Transport Coefficients

Mean-free-path expressions are discussed in Ref. 8. Here we present the results needed for our treatment of the scaling laws. We do not use the subscript f in this appendix.

The viscosity of a fluid expresses its ability to exert shear forces and is defined by

$$P_{xy} = -\mu \frac{\partial v_y}{\partial x} \quad , \tag{D.1}$$

where P_{xy} is xy-component of the fluid stress tensor, which is the transverse force per unit area or the transverse momentum flux, μ is the viscosity, and v_y is the y-component of the fluid velocity.

Mean-free-path arguments for the value of μ are based upon kinetic theory and the assumption that, on the average, the molecules of the fluid have properties characteristic of the location of their last collision. This leads to the expression

$$\mu = \xi_\mu \rho \bar{v} l \quad , \tag{D.2}$$

where ξ_μ is a constant (~0.3 - 0.4), ρ is the mass density of the fluid, $\bar{v}$ is the average speed of the molecules, and l is the mean-free-path between molecular collisions. Simple kinetic theory arguments give

$$\bar{v} \sim \sqrt{\frac{k_B T}{m}} \quad , \tag{D.3}$$

where k_B is the Boltzmann constant, T is the absolute temperature, and m is the molecular mass. Furthermore, the mean-free-path is given by

$$l \sim \frac{1}{n \sigma_c} \quad , \tag{D.4}$$

where n is the number density of molecules and σ_c is their total collision cross section.

The kinematic viscosity is defined by

$$\nu \equiv \mu/\rho \quad . \tag{D.5}$$

Putting the above expressions together yields

$$\nu \sim \sqrt{\frac{k_B T}{m}} \frac{1}{n\sigma_c} \quad . \tag{D.6}$$

The ideal gas equation of state gives n as a function of P and T

$$n = \frac{P}{k_B T} \quad , \tag{D.7}$$

and then we have

$$\nu = \nu_s \left[\frac{T}{T_s}\right]^{3/2} \left[\frac{P_s}{P}\right] \quad , \tag{D.8}$$

where the subscript s refers to some set of standard conditions. This is the expression used in (2.19). From (D.6), we expect that

$$\nu_s \sim \frac{1}{m^{1/2}\sigma_c} \quad . \tag{D.9}$$

This can be used as a guide in selecting gases.

The thermal conductivity k of a fluid is defined by

$$H_x = -k \frac{\partial T}{dx} \quad , \tag{D.10}$$

where $\vec{H}$ is the heat flux. Mean-free-path arguments yield the expression

$$k = \xi_k \rho \bar{v} \, l \, c_{vt} \quad , \tag{D.11}$$

for molecules with no thermally excited internal degrees of freedom. In this expression, ξ_k is a constant (~5/2) and c_{vt} is the contribution of the translation degrees of freedom of the molecule to the specific heat at constant volume. If the specific heat has a contribution from internal degrees of freedom c_{vi} then

$$k = \rho\bar{v}l(\xi_k c_{vt} + c_{vi}) \quad . \tag{D.12}$$

We have assumed that the specific heat is independent of temperature. For simplicity we will use (D.11) rather than (D.12) in what follows. The quantity ρc_{vt} is the heat capacity per unit volume of the gas; for an ideal gas, this is 3/2 nk_B. Putting this into (D.11) and using (D.3) and (D.4) gives

$$k = k_s \left[\frac{T}{T_s}\right]^{1/2} \quad , \tag{D.13}$$

where again

$$k_s \sim \frac{1}{m^{1/2}\sigma_c} \quad . \tag{D.14}$$

This is the expression used in (2.20).

The thermal diffusivity is defined by

$$\alpha = \frac{k}{\rho c_p} \quad . \tag{D.15}$$

We assume that ρc_p = 5/2 nk_B in accordance with the discussion of ρc_{vt} above. Then, using (D.7) for n, we have

$$\alpha = \alpha_s \left[\frac{T}{T_s}\right]^{3/2} \left[\frac{P_s}{P}\right] . \qquad (D.16)$$

This is the expression used in (2.21).

Equation (D.14) is an important guide in a search for gases that have low thermal conductivity and are therefore desirable for use in scaling. It states that we should seek a gas the molecules of which are massive and which have a large collision cross section.

Appendix E. Doghouse Modeling

The results described in detail in Sec. 3 can be tested by comparing the thermal performance of a small-scale structure with that of a full-scale one. Such a test is discussed in this appendix. For simplicity, we have chosen a cubic box having six identical sides--a doghouse--as our structure. One vertical side of the box is covered with electrical heaters in order to simulate the incidence of solar energy. We present below the design considerations, instrumentation, mode of operation, and data analysis for modeling such a structure. This exercise illustrates what must be done to model a realistic structure as well as serving as a test of our scaling relations. Throughout this appendix we will use the mean-free-path expressions for the transport coefficients derived in Appendix D. However, more accurate design parameters will be obtained if semi-empirical fits to the observed values of these coefficients are used. This technique will be reported in a subsequent paper.

The results of Sec. 3 plus considerations of cost, ease of handling, etc., suggest that SF_6 be used as the atmosphere in the small-scale model. This choice dictates the parameters to be used in Eqs. (3.22) - (3.26) for scaling variables. These are given in Table 3.2.

The next design choice is that of the operating pressure and temperature of the small-scale model. Here, considerations of time scale and temperature swing are dominant. The time scale for the small-scale model is given by

$$\tau = 1.85\ p\ t^{-13/2}\ , \qquad \text{(E.1)}$$

for an SF_6 atmosphere. Since we want a small value of τ, this suggests that we work at low pressure and/or high temperature. However, the amplitude of the temperature swing is given by

$$\delta = 0.161\ p^{-2}\ t^{23/2} \quad , \tag{E.2}$$

and keeping this number reasonable puts limits on the values of p and t. We choose $\delta = 10$ as a practical maximum value of δ thus relating p to t through (E.2). Cost considerations limit the value of p to the neighborhood of one, $0.75 < p < 1.25$. In what follows, we choose $p = 1$. However, p might be changed slightly in the field in order to fine-tune the system. Equation (E.2) then yields $t = 1.43$ or $T_0' = 146°C$ (295°F).

The parameters for the walls are determined by Eqs. (3.22) and (3.23) plus the above choices. We have $\kappa_w = 0.661$ and $\gamma_w = 2.34$. In Table E.1 we list the values of the thermal conductivity and heat capacity per unit volume for various materials. No two materials in this table have the proper ratios κ_w and γ_w. We solve this problem by making each wall out of two different materials. This will result in walls that have the proper static properties but have dynamic properties that are not matched. We hope that the mismatch is small. This hope can be checked quantitatively once the design parameters are chosen.

In accordance with the preceding discussion, we seek two two-material walls, made from the materials listed in Table E.1, the thermal conductivities and heat capacities of which have the given ratios κ and γ (we drop the subscript "w"). We denote the materials in the full-scale wall by 1 and 2 with thicknesses proportional to y and 1-y respectively, (see Fig. E.1). We denote the materials in the small-scale wall by 1' and 2' with thicknesses proportional to y' and 1-y' respectively. The thermal resistivity and heat capacity per unit volume of the full-scale wall are given by

$$C = y\ C_1 + (1-y)\ C_2 \quad , \tag{E.3}$$

$$R = y\ R_1 + (1-y)\ R_2 \quad , \tag{E.4}$$

and those of the small-scale wall by

$$C' = y' C_1' + (1-y') C_2' \quad , \tag{E.5}$$

$$R' = y' R_1' + (1-y') R_2' \quad . \tag{E.6}$$

In these equations, we have used resistivities $R = 1/k$ rather than conductivities since they are additive, as are the heat capacities. If we use $C' = \gamma C$ and $R' = R/\kappa$, then Eqs. (E.3) - (E.6) are a two-by-two system of linear equations for y and y' in terms of γ, κ, and the material parameters. These equations can be solved and if y and y' lie in the physical range between zero and one, then we have an acceptable combination of materials. More than 50,000 combinations of materials can be chosen from the list in Table E.1, and many of them pass the test. A more efficient method of choosing materials is the graphical method, which we now describe.

If we take Eqs. (E.3) and (E.4) and plot C as a function of R then we see that these equations are just a parametric representation of the straight line segment from the point (R_1, C_1) to the point (R_2, C_2) on the C vs. R plane. Any point on this line segment is a possible value of R and C. On the other hand, if we take Eqs. (E.5) and (E.6) and use $C' = \gamma C$ and $R' = R/\kappa$, then we see that it represents a straight line segment between the point $(\kappa R_1', C_1'/\gamma)$ and the point $(\kappa R_2', C_2'/\gamma)$ on the C vs. R plane. An acceptable combination of materials is represented by an intersection of these two line segments. Thus, in the graphical method, one plots the two sets of points (R_i, C_i) and $(\kappa R_i, C_i/\gamma)$, where i ranges over the materials of Table E.1. One joins the pairs of points in each set with straight lines and looks for intersections between the lines of the two sets. Most of this procedure can be carried out by eye and it leads to a rapid identification of

acceptable combinations of materials. This method has the further advantage that near-miss combinations of materials can also be easily identified.

The graphical method has been used to select plywood as the single component of the walls of the full-scale model. The walls of the small-scale model are 34% corkboard and 66% NEMA G-10. This leads to the values $k = 0.674$ and $\gamma = 2.26$, which is a near miss. However, uncertainties in material parameters more than mask the discrepancy.

The dynamic response of the two walls will be different due to their different internal structure. We can quantify this difference by considering the response of the wall to an applied temperature with a harmonic dependence upon time. We construct the wall in a symmetric fashion with two sheets of material 1 on the outside, each having a proportional thickness y/2, and one sheet of material 2 on the inside having a proportional thickness 1-y, (see Fig. E.1). A temperature variation $T_o\, e^{-i\omega t}$ is applied to the right-hand side while the temperature is held constant on the left-hand side. The heat flux on the left-hand side is given by

$$J_o = -\frac{k_w}{L}\, \chi_o\, T_o\, e^{-i\omega t} \quad , \tag{E.7}$$

and that on the right-hand side by

$$J_1 = -\frac{k_w}{L}\, \chi_1\, T_o\, e^{-i\omega t} \quad . \tag{E.8}$$

The factor k_w/L in these expressions is just the wall U-value; χ_o and χ_1 are dimensionless, frequency-dependent response factors normalized to one at zero frequency. Solving the heat equation yields the following expressions for the χ's:

For a single-material wall

$$X_o = \frac{K}{\sinh K} \quad , \tag{E.9}$$

$$X_1 = K \coth K \quad , \tag{E.10}$$

where $K^2 = -i\omega\tau_w$ and $\tau_w = C_w L_w^2/k_w$.

For the three-layer, two-material, wall

$$X_o = \frac{k_1 K_1}{k_w} \cdot \frac{1}{\Delta} \quad , \tag{E.11}$$

$$X_1 = \left[\frac{1}{2} \left(\frac{k_1 K_1}{k_2 K_2} + \frac{k_2 K_2}{k_1 K_1} \right) \sinh X_1 \sinh X_2 + \cosh X_1 \cosh X_2 \right] X_o \quad ,$$

where

$$\Delta = \frac{1}{2} \left[\left(\frac{k_1 K_1}{k_2 K_2} + \frac{k_2 K_2}{k_1 K_1} \right) \cosh X_1 + \left(\frac{k_1 K_1}{k_2 K_2} - \frac{k_2 K_2}{k_1 K_1} \right) \right] \sinh X_2 + \sinh X_1 \cosh X_2 \quad , \tag{E.13}$$

and $X_1 = K_1 y$, $X_2 = K_2(1-y)$ with $K_j^2 = -i\omega\tau_w (C_j/C_w)(k_w/k_j$ and C_w and k_w are given by (E.3) and (E.4). These expressions are compared in Table E.2 for various values of $\omega\tau_w$ for the one- and two-material walls described above. Note that scaling implies that the comparison should be made at equal values of $\omega\tau_w$. From this table we see that there is fairly good agreement between the response factors over a wide range of $\omega\tau_w$. It is clear from this table that case II (corkboard on the outside) is a better approximation to case I (single material) than case III

(corkboard on the inside). Thus, the walls of the full-scale box should be plywood of thickness L_w; the walls of the small-scale box should be a layer of NEMA G-10 of thickness 0.66 L_w' with a layer of corkboard on each side of thickness 0.17 L_w'. Scaling then implies that $L_w' = \ell L_w$ with $\ell = 0.225$. Note that we are using full three-dimensional scaling so that $L_f' = \ell L_f$. The overall size of the boxes and the thicknesses of their walls are determined by L_f and L_w--these are free parameters which can be chosen to simplify the construction of the boxes.

The time scale for the full-scale plywood box is given by

$$\tau_w = \frac{C_w L_w^2}{k_w} = 4.4 \left(\frac{L_w}{5\ \text{cm}}\right)^2 \text{ hrs} \quad . \tag{E.14}$$

The time scale for the small-scale model is $\tau_w' = \tau\tau_w$ with $\tau = 0.179$ for our choice of parameters. Tests of scaling for time-dependent phenomena should be run at frequencies such that

$$\omega\tau_w = 0,\ 1,\ 10 \quad . \tag{E.15}$$

Note that for $\omega\tau_w = 1$ and a 5 cm-thick wall we have a period of 27 hours. While the tests might best be run at a single frequency it is probably just as good to use a square-wave power input the fundamental frequency of which satisfies (E.15).

The power level for the full-scale model is dictated by its total heat capacity and the desired rate of temperature change. The six-sided plywood cube has a total heat capacity

$$C_{tot} = 2.6 \times 10^5 \left(\frac{L_f}{1\ \text{m}}\right)^2 \left(\frac{L_w}{5\ \text{cm}}\right) \frac{\text{J}}{\text{K}} \quad .$$

For a rate of temperature change T, the total power should be

$$P_{tot} = 360 \left(\frac{L_f}{1\ m}\right)^2 \left(\frac{L_w}{5\ cm}\right) \left(\frac{T\ hr}{5\ K}\right) w \ . \qquad (E.16)$$

All of this heat will not go into the walls, but this expression will still yield an estimate of the total power needed. The total power in the small-scale model scales as $P'_{tot} = \delta\ t^3\ \ell^2\ P_{tot}$ with $\delta\ t^3\ \ell^2 \simeq 1.5$ for our choice of parameters. Thus, both of these power levels are well below 1 kw for a reasonable choice of sizes and are therefore easily manageable.

Both full- and small-scale models should be instrumented so that the temperature distributions throughout their volumes can be compared. This must be done in the least intrusive fashion possible. We envision a 3x3x3 array of thermistors sensing the temperature throughout each volume. If these temperatures are sampled at a frequency ten times that of the power input we have 270 data points per model. Good statistics can then be built up by signal-averaging techniques. In this way, a digestible amount of good quality data can be generated.

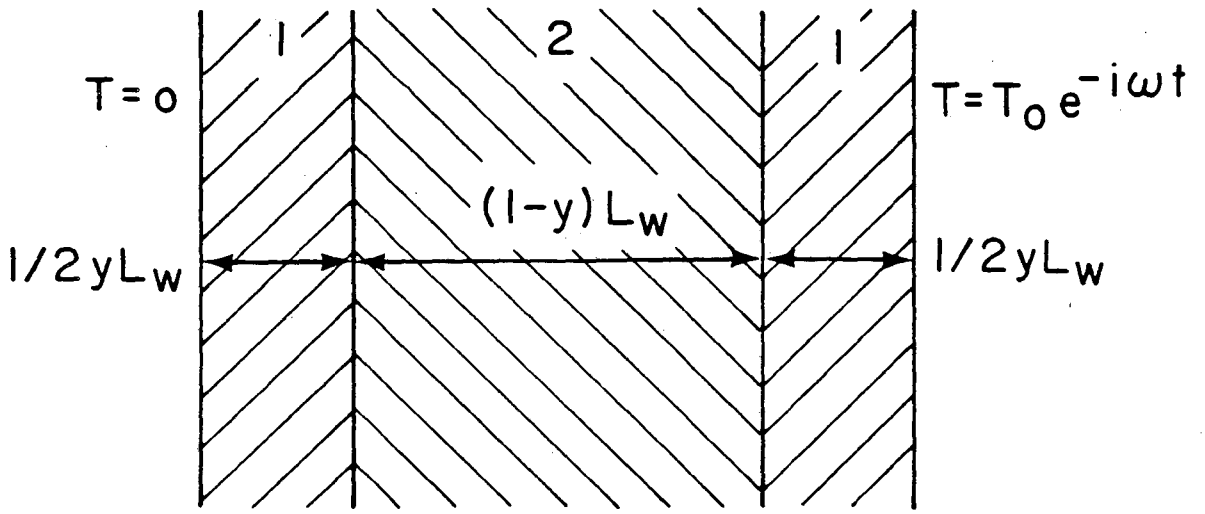

XBL 8110-1452

Fig. E.1. Structure of two-material, three-layer wall.
Material 1 is split into two symmetrical layers about one layer of material 2. Dimensions are given as fractions of the total width L_w.

Table E.1. Thermal conductivities and heat capacities per unit volume for selected materials.

Material	k $[\frac{W}{mK}]$	C $[\frac{kJ}{m^3K}]$
Gypsum board	0.170	872
Fiberglass insulation	0.0397	29.5
Plywood	0.138	866
Paper	0.100	1240
Asphalt shingle	0.145	979
White pine	0.120	1260
Fiberboard	0.0580	602
Corkboard	0.0400	376
Styrofoam	0.0300	252
Nylon-6	0.290	1920
Concrete	0.420	1350
Aluminum (6061)	171	2610
Copper (OFHC)	391	3430
Lead (common)	33.9	1480
NEMA G-10	0.294	2772
Epoxy (unfilled)	0.350	2180
Teflon	0.240	2310
Kapton	0.170	1550
Steel (C1015)	47.0	3450
Graphite	150	2810
Hard rubber	0.121	1900

Table E.2. Amplitudes and phases of the response factors χ_0 and χ_1 for three wall structures. Case I: single-material wall. Cases II and III: two-material wall (34% corkboard, 66% NEMA G10) in three symmetrical layers (see Fig. E.1). Case II has corkboard on the outside and Case II NEMA G10 on the outside.

Case	I		II		III	
$\omega\tau_w$	χ_0	χ_1	χ_0	χ_1	χ_0	χ_1
0.01	(1.00, 0.00)	(1.00, 0.00)	(1.00, 0.00)	(1.00, 0.00)	(1.00, 0.00)	(1.00, 0.00)
0.1	(1.00, 0.02)	(1.00,-0.03)	(1.00, 0.02)	(1.00,-0.03)	(1.00, 0.01)	(1.00,-0.04)
1	(0.99, 0.17)	(1.07,-0.31)	(0.98, 0.24)	(1.08,-0.23)	(1.00, 0.06)	(1.10,-0.41)
10	(0.67, 1.44)	(3.15,-0.81)	(0.43, 1.46)	(2.07,-0.31)	(0.96, 0.58)	(4.60,-1.19)
100	(0.02, 0.00)	(10.00,-0.79)	(0.02,-2.04)	(2.84,-0.48)	(0.16,-2.34)	(22.64,-0.79)

References

1. J.W. Drysdale, "Design of Buildings for Hot Climates," J. Inst. Heat. Vent. Eng. 17 467 (1950); 18, 401 (1951).

2. K.I. Parczewski and P.N. Renzi, "Scale Model Studies of Temperature Distributions in Internally Heated Enclosures," ASHRAE Transactions 69, 453 (1963).

3. J.M.F. Vickers, "Thermal Scale Modeling," Astronautics and Aeronautics, May 1965, 34.

4. R.L. Shanon, "Thermal Scale Modeling of Radiation - Conduction - Convection Systems," J. of Spacecraft and Rockets 10, 485 (1973).

5. J.G. Thompson, D. Han, and N.Z. Azer, "Design and Verification of a Thermal Scale Model for Environmental System Energy Studies," Paper presented at the ASHRAE Annual Meeting and to be published in ASHRAE Transactions 87, part 2 (1981).

6. F. Kreith, Principles of Heat Transfer, (Intext Educational Publishers, New York, 1973).

7. S. Chandrasekhar, Hydrodynamic and Hydromagnetic Stability, (Oxford University Press, London, 1961), p. 16; E.A. Spiegel, "Convection in Stars: I. Basic Bousinesq Convection," Ann. Rev. of Astronomy and Astrophysics 9, 323 (1971); S. Ostrach, "Natural Convection in Enclosures," Adv. in Heat Transfer, Vol. 8 (Academic Press, New York, 1972).

8. E.H. Kennard, Kinetic Theory of Gases, (McGraw-Hill Book Co., Inc., New York, 1938); J.O. Hirschfelder, C.F. Curtis, and R.B. Bird, Molecular Theory of Gases and Liquids, (John Wiley and Sons, Inc., New York, 1954).

9. A.L. Horvath, Physical Properties of Inorganic Compounds, (Crane-Russack, New York, 1975). Note that the thermal conductivity of SF_6 given in this reference is in error and the value given in Ref. 10 should be used.

10. The Matheson Company, Inc., The Matheson Gas Data Book (The Matheson Company, Inc.) p. 649-654.

11. D.E. Gray, Ed., American Institute of Physics Handbook, Third Edition, (McGraw-Hill Book Co., New York, 1972) p. 4-149, Y.S. Touloukian et al., Thermophysical Properties of Matter, vols. 3, 6, 11, (Plenum, New York, 1970).

12. Handbook of Chemistry and Physics, 61st Edition, p. E2 (CRC Press, Boca Raton, Fla., 1980).

TECHNICAL INFORMATION DEPARTMENT
LAWRENCE BERKELEY LABORATORY
UNIVERSITY OF CALIFORNIA
BERKELEY, CALIFORNIA 94720